Geophys. J. R. astr. Soc. (1975) **40**, 1–21

A Numerical Model of the Vertical Circulation of Tidal Estuaries and its Application to the Rotterdam Waterway

Peter Hamilton

(Received 1974 October 7)*

Summary

A two-dimensional numerical model has been developed to represent the vertical structure of current and salinity along an estuary of varying width and depth but with a rectangular cross-section. The governing equations, which express the conservation of volume, momentum and salt content, are solved by a finite difference initial-value method. The finite difference grid is arranged to cover the vertical profile of the estuary so that the free surface moves vertically through the grid points. Thus the surface elevation and the profiles of current and salinity are determined throughout the tidal period as the equations are integrated stepwise through time.

The model has been applied to the Rotterdam Waterway and the resulting distributions have been compared with field data from surveys by the Rijkswaterstaat of the Netherlands, made available for this study by the late Dr J. J. Dronkers. Reasonable agreement has been obtained and to this extent the ability of the model to reproduce the general features of estuarine circulation has been established.

1. Introduction

The vertical circulation of a coastal plain estuary is a function of the internal dynamics governed by factors such as the local horizontal density gradient, geometry of the channel and the strength of mixing and Reynold stresses; and also of external time-dependent forcing; i.e. the external tide, the riverflow and meteorological conditions. The time-dependent response of an estuary to such forcings has only been partly explored. The steady state has been studied in the theoretical work of Hansen & Rattray (1965) which showed the importance of the horizontal density gradient in producing a characteristic shear in the horizontal current which in many cases produces a landward flow near the bed and a seaward flow at the surface. The magnitude of this flow, usually called a density current, and its effect on the vertical distribution of salinity is strongly dependent on the values of the eddy diffusion and viscosity coefficients (Hansen & Rattray 1965). For many estuaries, the variations in current and salinity produced by the tide are not only of interest in themselves but are also important in determining the distribution and flushing of introduced pollutants. The tide in many cases is also the primary source of energy for turbulent mixing and stresses.

* Received in original form 1974 May 2

The time-dependent equations which govern the distribution of salinity and current have not been solved analytically, even for a uniform channel, and given the non-linearities of the problem it was decided to investigate the behaviour of a partially-mixed coastal plain estuary by the use of a numerical model. This paper is primarily concerned with the principles of computation. The use of the model to determine the effect of the tide, the riverflow and various functional forms for the eddy coefficients will be discussed elsewhere, however, the application of the model to the Rotterdam Waterway is presented here to show that the model is capable of a reasonable representation of salinity and currents throughout the tidal period in a natural estuary (Section 7). The Rotterdam Waterway was chosen because of the availability of high quality data and also because it has been subject to numerical modelling and some comparison can be made between the various types of models (two layer, Vreugdenhill 1970; and vertically integrated, Stigter & Siemons 1967).

The application of numerical models to estuaries has taken two forms: (a) in which main interest is the propagation of a tidal wave (Dronkers 1964; Rossiter & Lennon 1965) or the interaction of the tide and an external surge (Rossiter 1961) in an estuary; and (b) in which the interest is in the mixing of salt- and freshwater within an estuary (Stigter & Siemons 1967; Williams & West 1973; Mollowney 1973).

All the above models are one-dimensional in that they use depth integrated forms of the equations of conservation of volume, momentum (a), and salt content (b). The extension to two horizontal dimensions of case (a) has been carried out by Leendertse (1967) and Heaps (1969) among others and is used to study the dynamical response of coastal seas to external wind and pressure fields-storm surge phenomena. Leendertse (1970) has also extended case (b) to bays and coastal seas.

All the models mentioned so far are not able to offer any elucidation of the vertical structure of the current or salinity distribution. Vreugdenhill (1970) has developed a two-layer model and applied it to the Rotterdam Waterway which calculates the mean velocities of the two layers, the upper being freshwater and the lower having the density of the seawater at the mouth. In the case where no mixing between the layers is allowed, the form of the velocity profile is derived separately from assumptions about the turbulent stresses. In the case where mixing is allowed between the layers a salinity profile can also be derived. Difficulties with the tidal variation of the interface and a satisfactory formulation of the boundary conditions at the interface, particularly in the case with mixing, were found, Hobbs & Fawcett (1973) use a two-dimensional grid arranged in a vertical plane and solve the equations of conservation of salt, temperature and various pollutants for the River Tees, where the velocities and tidal elevations are prescribed by curve fitting techniques to experimental data.

Mention should be made of the numerical modelling of the vertical structure of smaller scale flows by the marker and cell technique (MAC) which have been used to simulate tank experiments (Daly & Pracht 1968; Chan & Street 1970; Young & Hirt 1972). The model described below has some similarities with these models. A grid arranged in the vertical plane is used, but the free surface is given directly by the governing equations and not defined by marker particles. The flow is turbulent and a rather more complex geometry is used than is usual in these type of models. Also special boundary conditions such as the imposed tide at the mouth and the frictional effect of the bed on the fluid are required. The numerical method, which is a one time step explicit scheme, is similar to that considered by Heaps (1969).

An important feature is the numerical approach to the basic equations, which considers the depth dependent variables, velocity and salinity, as *continuous*. This is in contrast with layered models which have hitherto been used for estuaries in which the equations of momentum and salt conservation are integrated over the separate layers (two or more) and exchange of momentum and salt between the layers is parameterized in terms of the mean velocities and salinities of the layers. A con-

tinuum approach allows better treatment of the surface and bottom boundary conditions, which is an important feature of the model.

2. Mathematical description of the model

The governing equations of the model using the Boussinesq approximation for a narrow channel with a rectangular cross-section are:
the equations of continuity:

$$\frac{\partial \zeta}{\partial t} + \frac{1}{b}\frac{\partial}{\partial x}\left[b\int_{-\zeta}^{h} u\,dz\right] = 0 \tag{1}$$

$$\frac{\partial}{\partial x}(bu) + b\frac{\partial w}{\partial z} = 0 \tag{2}$$

salt conservation:

$$\frac{\partial s}{\partial t} + u\frac{\partial s}{\partial x} + w\frac{\partial s}{\partial z} - \frac{\partial}{\partial z}\left(K_z\frac{\partial s}{\partial z}\right) - \frac{1}{b}\frac{\partial}{\partial x}\left(bK_x\frac{\partial s}{\partial x}\right) = 0 \tag{3}$$

and momentum conservation:

$$\frac{\partial u}{\partial t} + u\frac{\partial u}{\partial x} + w\frac{\partial u}{\partial z} = \underline{-ag(z+\zeta)\frac{\partial s}{\partial x} - g\frac{\partial \zeta}{\partial x}} + \frac{\partial}{\partial z}\left(N_z\frac{\partial u}{\partial z}\right) \tag{4}$$

where the notation is as follows:

x, z co-ordinates in the plane of the undisturbed water surface (positive seawards) and vertically downwards, respectively,

t time,

ζ elevation of the water surface above the undisturbed plane,

u, w velocity components in the directions x and z respectively,

s salinity,

h, b depth and width of the channel, respectively (functions of x only),

N_z coefficient of vertical eddy viscosity,

K_z, K_x coefficients of vertical and horizontal eddy diffusivity, respectively,

g acceleration due to gravity.

Salinity is connected to density ρ by a linear equation of state:

$$\rho = \rho_0(1+as) \tag{5}$$

with ρ_0 = density of freshwater

and $a = 7{\cdot}8\times10^{-4}$ (derived from σ_t tables).

This is usually regarded as a satisfactory approximation on account of the large horizontal changes in salinity which occur in estuaries (Bowden 1967).

If the estuary is considered as a channel of length L then the boundary conditions at the head of freshwater flow are given:

$$s(x, z, t) = 0 \qquad \text{at } x = 0 \tag{6}$$

$$u(x, z, t) = \frac{q}{(h+\zeta)b} \qquad \text{at } x = 0, \forall z, t. \tag{7}$$

where q is the riverflow, usually a constant, ($m^3 s^{-1}$). At the mouth the elevation is given in the form of a tidal input and also the salinity is prescribed:

$$\zeta(x, t) = A(t) \qquad \text{at } x = L \tag{8}$$

$$s(x, z, t) = s_0 \qquad \text{at } x = L. \tag{9}$$

If the tide is semi-diurnal, $A(t) = -A_0 \cos \sigma t$, $\sigma = 2\pi/T$, where A_0 is the tidal amplitude and T the tidal period, 12·42 hr. If the channel is extended out to sea then s_0 may be regarded as a constant, representative of the nearby coastal sea, however if this is not done it may be necessary to prescribe s_0 as a function of z and t.

There is no salt flux through the water surface or through the bed of the estuary, therefore

$$K_z \frac{\partial s}{\partial z} = 0 \qquad \text{at } z = h \text{ and } -\zeta, \forall x, t. \tag{10}$$

Surface wind stress is neglected;

$$N_z \frac{\partial u}{\partial z} = 0 \qquad \text{at } z = -\zeta, \forall x, t, \tag{11}$$

and the stress of the fluid on the bed is assumed to obey the quadratic friction law, hence

$$-N_z \frac{\partial u}{\partial z} = k|u_\Delta|u_\Delta \qquad \text{at } z = h, \forall x, t \tag{12}$$

where k is a constant usually taken to be 0·0025 and

$$u_\Delta = u(x, z, t) \qquad \text{at } z = h - \Delta. \tag{13}$$

Thus the bottom stress is related to the velocity at a distance Δ above the bottom. Δ can be considered to be representative of the frictional layer just above the bottom and this is taken to be 1 metre (Pritchard 1956).

Mention should be made of the approximation made in deriving the underlined terms in equation (4) from the hydrostatic approximation. Strictly, the derivation leads to

$$\frac{\partial p}{\partial x} = g(z+\zeta)\frac{\partial \bar{\rho}}{\partial x} + g\bar{\rho}\frac{\partial \zeta}{\partial x} \tag{14}$$

where p is the pressure and $\bar{\rho}$ the mean density of a water column stretching from the surface to depth z. Thus

$$\bar{\rho}(x, t) = \frac{1}{z+\zeta}\int_{-\zeta}^{z} \rho(x, z, t)dz. \tag{15}$$

The approximation is to replace $\bar{\rho}$ by ρ in (14), apply (5) and set $\rho/\rho_0 = 1$. The error introduced will be very small compared with the other approximations introduced unless the estuary is highly stratified when (14) may have to be used. The advantage of this formulation is that it saves a number of numerical integrations which would be associated with equation (15).

3. The finite difference grid

The finite difference grid and the method of notating the grid points are similar to that used by Heaps (1969). The grid is shown in Fig. 1 and the grid points are divided into two types, salinity points (+) and velocity points (·), both similarly numbered by the parameter i. n is the number of salinity points in a column and a column of salinity points is defined by two parameters, p and $k = 2p$, where

$$p = \text{int}\left(\frac{i-1}{n}\right) + 1. \tag{16}$$

A column of $n-1$ velocity points is defined by the parameters p and $k = 2p-1$ and thus P is the total number of salinity or velocity columns used in the grid. The grid is arranged to cover the profile of the estuary with the x-axis passing through the salinity points given by

$$i = i_g(p) = (p-1)n+l \qquad \text{for } p = 1, \ldots, P \tag{17}$$

where $l(>0)$ is the x-axis parameter, taken as sufficiently large such that the top of the grid is always above the water surface ($l = 3$ in Fig. 1).

The quantities associated with the equations (1)–(4) are defined with respect to the grid by

$s = s_i$, $w = w_i$, $N_z = N_{z,i}$, $K_z = K_{z,i}$ at a salinity point i,

$u = u_i$ at a velocity point i,

$\zeta = \zeta_p$ at a salinity column p,

$K_x = K_{x,p}$ at a velocity column p,

$b = b_k$, $h = h_k$ at all columns $k(= 1, \ldots, 2P)$

where s_i denotes the value of s at salinity grid point i, etc.

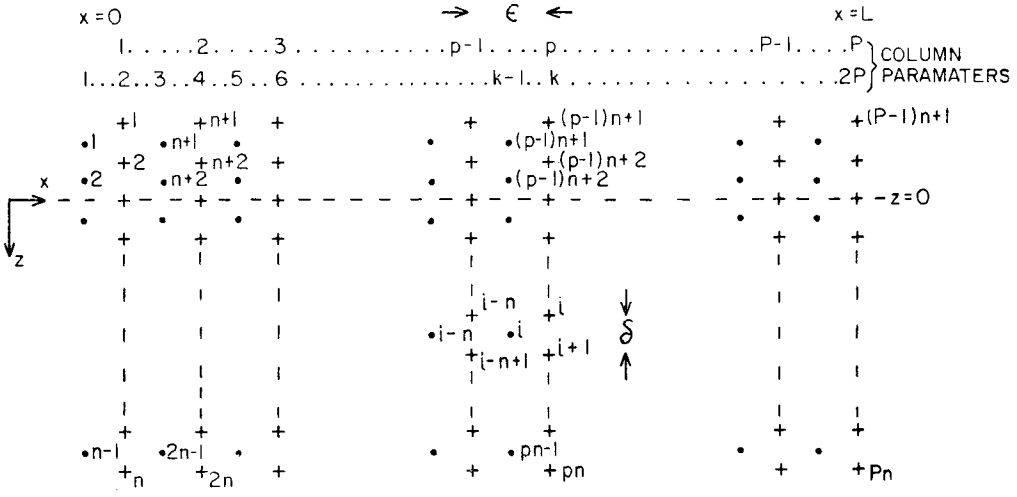

FIG. 1. The finite difference grid. +, salinity point; ·, velocity point.

The grid points that define the position of the bed and the free surface with respect to a column of grid points, k, are respectively defined by

$$\left.\begin{aligned} i = i_b(k) &= i_g(p) + \text{int}\,(h_k/\delta) \quad \text{for } k = 2p \\ i = i_b(k) &= i_g(p) + \text{int}\,(h_k/\delta - \tfrac{1}{2}) \quad \text{for } k = 2p-1 \end{aligned}\right\} \tag{18}$$

for $p = 1, \ldots, P$, where δ is the vertical grid spacing, and

$$i = i_s(k) = i_g(p) - \text{int}\,(\zeta_k/\delta) \qquad \text{for } p = 1, \ldots, P, \tag{19}$$

where

$$\left.\begin{aligned} \zeta_k &= \zeta_p \quad \text{for} \quad k = 2p \text{ and } k = p = 1 \\ \zeta_k &= (\zeta_p + \zeta_{p-1} + \delta)/2 \quad \text{for} \quad k = 2p-1. \end{aligned}\right\} \tag{20}$$

Therefore $i_b(k)$ and $i_s(k)$ define the grid points just above the bottom and just beneath the surface respectively. Equations (10) and (11) assume that the free surface is nearly horizontal, however such an assumption is not necessary for the computational method. An assumption is made in the logic that the free surface elevation does not differ by more than the vertical grid spacing δ (say 2 m) between successive stations, horizontal spacing ε (say 2 km). A condition unlikely to be violated in nature. The bottom and surface are defined with respect to these grid points by

$$d_b(k) = \begin{cases} h_k - \big(i_b(k) - i_g(p)\big)\delta & \text{for} \quad k = 2p \\ h_k - \big(i_b(k) - i_g(p) + \tfrac{1}{2}\big)\delta & \text{for} \quad k = 2p-1 \end{cases} \tag{21}$$

which is the distance of the bed from the bottom grid point $i_b(k)$, and

$$d_s(k) = \zeta_k - \big(i_g(p) - i_s(k)\big)\delta, \tag{22}$$

where ζ_k is given by (20), which is the distance of the water surface from the grid point $i_s(k)$, (Fig. 2).

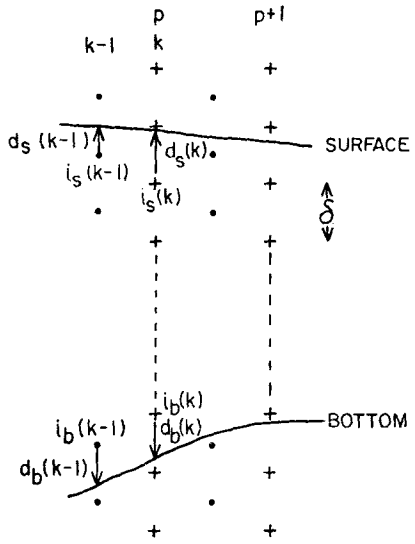

FIG. 2. A column of grid points showing the position of the free surface and bottom with respect to the grid points $i_s(k)$ and $i_b(k)$ by $d_s(k)$ and $d_b(k)$, respectively.

Therefore $i_s(k)$, $i_b(k)$, $d_s(k)$ and $d_b(k)$ define the boundaries of the grid and as the free surface moves through the grid points $i_s(k)$ and $d_s(k)$ will change with time. In the sections that follow the dependence of the above parameters on p and k will be implicit. The horizontal extent of the grid and thus the total number of grid points (nP) depends on the horizontal grid spacing, ε, chosen.

4. The finite difference equations

The basic differential equations (1), (2), (3) and (4) are now replaced by finite difference equivalents. The method is in essentials due to Heaps (1969) and uses forward and backward time differences and central differences in space except for the horizontal advective term in (3), which makes use of a form of upwind differencing. The finite difference equations relate ζ_p, s_i, v_i at time $t+\tau$ to the values at a preceding time, t, τ being the time step. The time dependence of the variables is denoted by the superscripts t and $t+\tau$:

$$\frac{\zeta_p^{\,t+\tau}-\zeta_p^{\,t}}{\tau}+\frac{1}{b_k}\left[\frac{b_{k+1}[u^t]_{p+1}-b_{k-1}[u^t]_p}{\varepsilon}\right]=0, \tag{23}$$

where $k=2p$ and $[u^t]_p$ represents the numerical integration of $\int_{-\zeta}^{h} u(x,z,t)dz$, on column p.

$$\frac{b_k(w^t_{i+1}-w^t_i)}{\delta}+\frac{(b_{k+1}u^t_{i+n}-b_{k-1}u^t_i)}{\varepsilon}=0 \tag{24}$$

$$\begin{aligned}\frac{s_i^{t+\tau}-s_i^t}{\tau}+\frac{1}{4\varepsilon}\;&[\alpha_{i+n}(s^t_{i+n}-s^t_i)+\alpha_i(s^t_i-s^t_{i-n})+(\alpha_{i+n}+\alpha_i)\Delta s]+w^t_i\frac{(s^t_{i+1}-s^t_{i-1})}{2\delta}\\&-\left[\frac{(K^t_{z,i+1}+K^t_{z,i})(s^t_{i+1}-s^t_i)-(K^t_{z,i}+K^t_{z,i-1})(s_i^{t+\tau}-s_{i-1}^{t+\tau})}{2\delta^2}\right]\\&-\frac{1}{b_k}\left[\frac{b_{k+1}K_{x,p+1}(s^t_{i+n}-s^t_i)-b_{k-1}K_{x,p}(s_i^{t+\tau}-s_{i-n}^{t+\tau})}{\varepsilon^2}\right]=0\end{aligned} \tag{25}$$

where $k=2p$, $\alpha_i=(u_i^t+u^t_{i-1})/2$ and

$$\Delta s=\begin{cases}s^t_{i+n}-s^t_i & \text{if}\quad \alpha_{i+n}+\alpha_i<0\\ s^t_i-s^t_{i-n} & \text{if}\quad \alpha_{i+n}+\alpha_i\geqslant 0.\end{cases} \tag{26}$$

$$\begin{aligned}&\frac{u_i^{t+\tau}-u_i^t}{\tau}+u_i^t\frac{(u^t_{i+n}-u^t_{i-n})}{2\varepsilon}\\&+\frac{(w^t_{i+1}+w^t_{i-n+1})(u^t_{i+1}-u^t_i)+(w_i^t+w^t_{i-n})(u_i^t-u^t_{i-1})}{4\delta}\\&=-ag\left(z_i+\frac{\zeta_p^{\,t+\tau}+\zeta_{p-1}^{t+\tau}}{2}\right)\left(\frac{s_i^{t+\tau}-s_{i-n}^{t+\tau}+s_{i-1}^{t+\tau}-s_{i-n+1}^{t+\tau}}{2\varepsilon}\right)\end{aligned}$$

$$-g\frac{(\zeta_p^{t+\tau}-\zeta_{p-1}^{t+\tau})}{\varepsilon}$$

$$+\frac{(N^t_{z,i+1}+N^t_{z,i-n+1})(u^t_{i+1}-u^t_i)-(N^t_{z,i}+N^t_{z,i-n})(u_i^{t+\tau}-u_{i-1}^{t+\tau})}{2\delta^2}, \qquad (27)$$

where z_i is the depth of velocity grid point i, i.e.

$$z_i = (i-i_g+\tfrac{1}{2})\delta. \qquad (28)$$

The equations are rearranged to give the variables at time $t+\tau$ in terms of the variables at time t. The equations are evaluated in the order presented above for increasing values i and p, thus the scheme is explicit. For example, the term $u_{i-1}^{t+\tau}$ in the difference form of $\partial/\partial z(N_z\partial u/\partial z)$ in (27) is known from a previous calculation. In evaluating equation (24) for a salinity column $k = 2p$, use is made of the boundary condition

$$w = 0 \quad \text{at} \quad z = h. \qquad (29)$$

Therefore at $i = i_b$, equation (24) becomes

$$w_i^t = \frac{d_b}{\varepsilon b_k}(b_{k+1}\,u^t_{i+n}-b_{k-1}\,u^t_i),\ i = i_b. \qquad (30)$$

At an interior grid point

$$w_i^t = w^t_{i+1}+\frac{\delta}{\varepsilon b_k}(b_{k+1}\,u^t_{i+n}-b_{k-1}\,u_i^t)$$

$$i = i_b-1, \ldots, i_s. \qquad (31)$$

Thus using (30) and (31) with i decreasing from bottom to surface w_i can be calculated for each salinity column, except for $p = P$.

The combination of upwind and central differences for the horizontal advective term was arrived at during the initial testing of the model. Upwind differencing biases the advective term towards the upstream side of the point considered. The idea is that the change in salinity at any point due to advection is brought about only by salt advected from upstream. It was found that use of the conservation form of equation (3) when modelled by the conservative second and fourth order methods of Crowley (1968) led to catastrophic instabilities which were not experienced when the advective form (3) was used. These instabilities associated with the conservation form of the equation can be eliminated by an adaptation of a procedure due to Young & Hirt (1972) in which after one complete cycle $s_i^{t+\tau}$ is recalculated using the updated values of $s_i^{t+\tau}$ and $u_i^{t+\tau}$ in the right-hand side of the equation. This of course increases the amount of computer time needed by approximately one-third. Returning to the advective form of the equation, various schemes were used to overcome physically unrealistic salinities which appeared during test runs with a channel of constant width and depth and an initial horizontal salinity gradient ($t = 0$) of $\partial s/\partial x = 1{\cdot}179‰\ \mathrm{km}^{-1}$. Salinities became negative near the head and greater than the sea mouth salinity s_0 near the mouth. The second and fourth order methods of Crowley (1968), nine point differencing schemes due to Fromm (1968) and Arakawa (1966) were tried without the desired improvement in the salinity. The most successful method which produced

acceptable salinities was the simple 'upwind' differencing scheme. The disadvantage of this method is that it introduces a large apparent horizontal diffusion coefficient (Roach 1972). To mitigate this effect the upwind scheme was linearly combined with a second-order centred scheme (Crowley 1968) to produce the final form of equation (25).

Writing the diffusion and friction terms in (25) and (27) in semi-implicit form removes stability restriction on N_z and K_z (Section 6) and test calculations showed that there was virtually no difference (for appropriate values of N_z and K_z) between using this semi-implicit method and the more usual totally explicit form for these terms.

A flow diagram of the computational scheme is given in Fig. 3. A few points should be noted:

(i) The initial values ζ_p^t, u_i^t, s_i^t at $t = 0$ have to be prescribed either from nature, in the case of the Rotterdam Waterway, or by an artificial set of values which are assumed after a number of run in tidal periods not to effect unduly the subsequent calculations.

(ii) At each time step the new values of $\zeta_p^{t+\tau}$ are used to define the free surface and a 'new' grid, i.e. i_s and d_s are recalculated using (19) and (22).

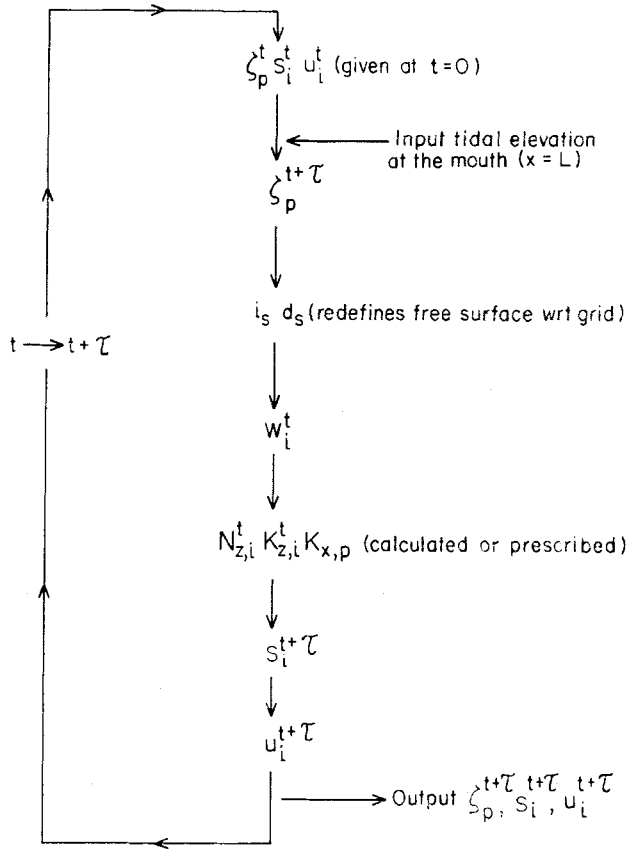

FIG. 3. Flow diagram showing the computational method.

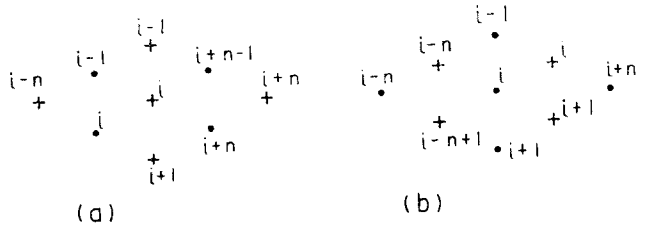

FIG. 4. Grid points which are needed to calculate $s_i^{t+\tau}$ from equation (25), (a), and $u_i^{t+\tau}$, from equation (27), (b).

The computer program was written in FORTRAN for an English Electric KDF9 installation of 26K storage capacity. The arrays corresponding to ζ_p, u_i, s_i were written to magnetic tape at every time step and the tape subsequently used to produce graphs of the tidal variation of surface and bottom salinities and velocities at various depths.

5. Modifications to the finite difference equations in the presence of a boundary

The finite difference equations (25) and (27) for each grid point i, require the values at five salinity points and four velocity points in the case of a salinity point and five velocity and four salinity points in the case of a velocity point, respectively. These are shown in Fig. 4.

At a grid point next to a boundary, free surface or bottom, values of s or u may not exist at some of these grid points. Therefore, values of s and u are extrapolated down below the bed and up above the surface, by the use of quadratic polynomials, to enable these grid points to have values assigned to them. Experience has shown (Chan & Street 1970; Nichols & Hirt 1971; Hamilton 1973) that accurate formulation of the boundary conditions is important in minimizing spurious instabilities. Hence the procedures for defining the position of the surface and bottom with respect to the grid (21, 22).

The boundary conditions (10) and (11) are used and N_z and K_z are taken to be finite at the surface and bottom thus

$$\left.\begin{aligned} \frac{\partial s}{\partial z} &= 0 \quad \text{at} \quad z = -\zeta \text{ and } h \\ \frac{\partial u}{\partial z} &= 0 \quad \text{at} \quad z = -\zeta \end{aligned}\right\}. \tag{32}$$

Consider three points $z = a, b$ and c with $a \leqslant b < c$, then if $f(z)$ has continuous first derivatives in the interval $[a, c]$ and $f'(a)$, $f(b)$ and $f(c)$ are known, then

$$f(z) = f(c) + \left(\frac{f(c)-f(b)}{C}\right)(z-c) + \frac{1}{2A-C}\left(f'(a) - \frac{f(c)-f(b)}{C}\right)(z-c)(z-b) \tag{33}$$

where $A = a-b$ and $C = c-b$. If $A = 0$ then (33) reduces to

$$f(z) = f(c) + \left(\frac{f(c)-f(b)}{C}\right)(z-c) + \left(\frac{f(c)-f(b)}{C^2} - \frac{f'(b)}{C}\right)(z-c)(z-b). \tag{34}$$

Thus (33) can be used to extrapolate s and u above the surface and s below the bottom. For example, at salinity point $i = i_s$, s_i, s_{i+1} and $\partial s/\partial z = 0$ at $z = -\zeta$ are known, so applying (33) with $A = -d_s$, $C = \delta$, $f'(a) = 0$, $f(b) = s_i$, $f(c) = s_{i+1}$, $a = -d_s$, $b = 0$, $c = \delta$, and $z = -\delta$, then

$$s_{i-1} = +2s_i - s_{i+1} + \frac{2\delta(s_{i+1} - s_i)}{(2d_s + \delta)}. \tag{35}$$

The numerical evaluation of the integral $\int_{-\xi}^{h} u dz$ in equation (23) is found by using the method of linearized splines (Birkhoff & Garabedian 1960; de Boor 1962). (33) and (34) are the basis and because quadratic splines are used only one boundary condition is needed, namely $\partial u/\partial z = 0$ at $z = -\zeta$, also the system of linear equations which connect the first derivatives can be rapidly solved as a recurrence relation. A system of cubic splines needs two boundary conditions and requires a tri-diagonal matrix equation to be solved, which would require more computer time. This method gives a value of the derivative u'_i at $i = i_b$ thus (34) can be used to find u_{i+1} by extrapolation and also $u_\Delta = u(x, h-\Delta, t)$ for use in the bottom friction equation (12). Each spline is separately integrated and the resulting integrations summed over the column of grid points to give the complete integral. The method is more accurate than a trapezium rule integration, considerably so when only 2 or 3 grid points are involved.

The term $\partial/\partial z(K_z \partial s/\partial z)$ represents the vertical diffusion of salt due to turbulence and it is important that this term should be accurately expressed in a finite difference formulation because there is no transport of salt through the boundary. A second-order derivative at grid point i, requires values at grid points i, $i+1$ and $i-1$. At the surface $i = i_s$, s_{i-1} exists because of the extrapolation procedures described above (equation (35)), but this is not considered to be accurate enough because the use of quadratic polynomials does not allow the definition of a second derivative. A fourth-order method using Taylor series expansions about the point $i = i_s$, considering s to be a continuous function of $z(C^3)$, is used to approximate $\partial^2 s/\partial z^2$, the diffusion term being approximated by $K_z \partial^2 s/\partial z^2$ near the surface. The result taking into account the boundary condition (32) is:

$$\left.\frac{\partial^2 s}{\partial z^2}\right|_{i=i_s} \simeq \frac{(8\delta^2 - 6d_s^2)s_{i+1} - (7\delta^2 - 3d_s^2)s_i - (\delta^2 - 3d_s^2)s_{i+2}}{\delta^2(3d_s^2 + 6\delta d_s + 2\delta^2)}. \tag{36}$$

Similar expressions exist for the second derivatives of u and s at $i = i_s$ and $i = i_b$, respectively. These results are incorporated into the finite difference equations (25) and (27) at boundary grid points. At the velocity point $i = i_b$, the effect of bottom friction is included and the finite difference representation of $\partial/\partial z(N_z \partial u/\partial z)$, taking into account (12), is:

$$\left(\frac{-k|u_\Delta|u_\Delta - N_z^t(d')[u_i^{t+\tau}(3\delta - 2d') - u_{i-1}^{t+\tau} 4(\delta - d') - u_{i-2}^{t+\tau}(2d' - \delta)]/2\delta^2}{d_b + d'}\right) \tag{37}$$

where

$$\left.\begin{aligned} d' &= d_b \text{ iff } d_b \geqslant \delta/2 \\ d' &= \delta/2 \text{ iff } d_b < \delta/2 \end{aligned}\right\} \tag{38}$$

and

$$\begin{aligned} N_z^t(d') = [&N^t{}_{z,i}(3\delta - 2d') + N^t{}_{z,i-1}(2d' - \delta) + N^t{}_{z,i-n}(3\delta - 2d') \\ &+ N^t{}_{z,i-n-1}(2d' - \delta)]/4\delta. \end{aligned} \tag{39}$$

The term is centred about the point $i = i_b$ if $d_b \geqslant \delta/2$, otherwise it is centred between $i = i_b$ and $i_b - 1$. This is to ensure that the denominator of (37) does not become too small, for if the bed of the estuary passes through $i = i_b$ such that $d_b = 0$, and as the boundary condition (12) always applies at the bottom, it becomes impossible to centre the frictional term about $i = i_b$ without making the denominator of (37) zero. Therefore when d_b is smaller than an arbitrary value, taken to be half the vertical grid spacing in (38), the frictional term is centred about a point above the bed to ensure that the finite difference form (37) does not become indeterminate. As an example, at the bottom grid point $i = i_b$, equation (27) becomes:

$$u_i^{t+\tau} = \left[u_i^t - \frac{\tau}{2\varepsilon} u_i^t (u^t{}_{i+n} - u^t{}_{i-n}) - \frac{\tau}{2\varepsilon} ag(z_i + (\zeta_p{}^{t+\tau} + \zeta_{p-1}^{t+\tau})/2)\right.$$

$$\cdot (s_i^{t+\tau} - s_{i-n}^{t+\tau} + s_{i+1}^{t+\tau} - s_{i-n+1}^{t+\tau}) - \frac{\tau}{\varepsilon} g(\zeta_p{}^{t+\tau} - \zeta_{p-1}^{t+\tau})$$

$$\left. + \frac{\tau}{d_b + d'} \left(-k|u_\Delta|u_\Delta + \frac{N^t{}_z(d')}{2\delta^2} (u_{i-1}^{t+\tau} 4(\delta - d') + u_{i-2}^{t+\tau} (2d' - \delta))\right)\right]$$

$$\Big/ \left(1 + \frac{\tau}{2\delta^2 (d_b + d')} N^t{}_z(d')(3\delta - 2d')\right), \tag{40}$$

where d' and $N_z^t(d')$ are given by (38) and (39) above and u_Δ is found from the interpolation procedures outlined above.

6. Stability

A stability analysis (Leendertse 1967; Morton 1971) of the linearized equations has been made to assess stability 'in the large', i.e. the boundary conditions are disregarded. The scheme is stable by the Von Neumann criterion (Richtmyer & Morton 1967) if

$$\tau < \frac{\varepsilon}{\sqrt{(2gH)}} \tag{41}$$

$$\frac{U\tau}{\varepsilon} < 1, \qquad \frac{W\tau}{\delta} < 1, \tag{42}$$

where H is the maximum depth and U and W are typical horizontal and vertical velocities respectively. These are only approximate relationships due to the difficulty of the mathematical analysis. Condition (41) can be obtained from dynamical reasoning about the propagation of one-dimensional waves in channels (Leendertse 1967). The interest in this scheme is the elimination of the dependence of τ on δ, as if (41) is fulfilled, then for typical values of U, W and δ (42) will always be satisfied. This seems to be the result of writing the diffusion and frictional terms in (3) and (4) semi-implicitly otherwise conditions similar to $\tau < \delta^2/N_z$ would be expected (Richtmyer & Morton 1967).

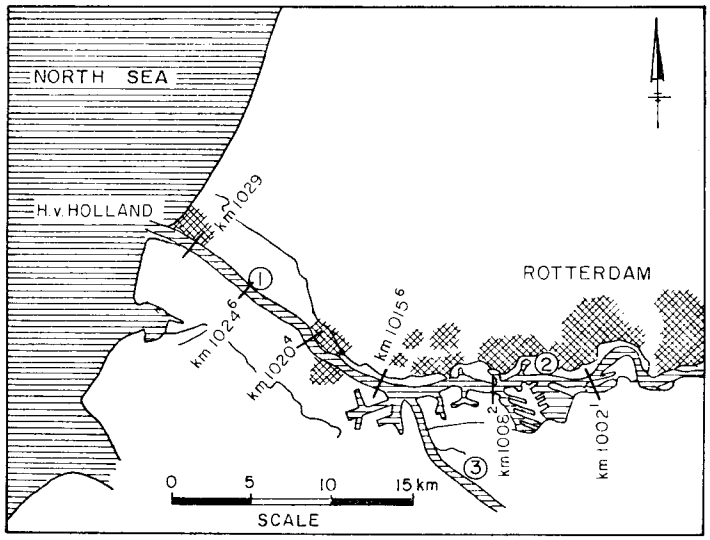

FIG. 5. The Rotterdam Waterway—1, Nieuwe Mass—2, Oude Maas—3. The km position of Sections 1, 2, 3, 4, 6 and 7 are shown, numbering from the mouth.

7. The Rotterdam Waterway

The Rotterdam Waterway is a man-made channel serving the port of Rotterdam and is the outlet of the River Rhine to the sea (Fig. 5). The Waterway has features which make it suitable for modelling. The channel is fairly regular in the region of the salt intrusion and is almost rectangular in cross-section, there are no tidal flats and the estuary can be considered as one channel. (The Rotterdam Waterway and Nieuwe Maas), the contribution to the flow by the Oude Maas can satisfactorily be neglected (Stigter & Siemons 1967). However, the extensive docks and harbours opening onto the Waterway affect the tidal regime and thus flow in the channel. The high freshwater flow from the Rhine (1000–1500 $m^3 s^{-1}$) determines the regime of the estuary which is highly stratified (over 10‰ in some places) with a strong density current circulation.

The Waterway is modelled by following the procedure of Stigter & Siemons (1967) and Vreugdenhill (1970) in that a channel of constant width and depth is used. To reproduce the tide correctly a channel length of about 100 km is required even though the length of the salt intrusion is only about 30 km. To save computer time it might have been possible to combine the two-dimensional model of the salt intrusion region with a one-dimensional tidal model of the upper reaches of the channel.

The model has been used to determine the tidal elevation, salinity and current for a tidal period corresponding to 0600–1900 hr on September 9, 1967 for the salt intrusion region. During this period measurements were taken by the Rijkswaterstaat at seven sections along the waterway (referenced by km 1029, km 1015·6, etc.) of current and salinity at four positions at each section, every half hour for the above period. Tidal elevations were also measured. The seaward boundary was assumed to be at km 1029. (Section 1) and the values of ζ and s were taken from the measurements. The initial values of salinity were taken from the data corresponding to 0600 hr, however, the elevation at all positions along the channel was taken to be that at Section 1 at 0600 hr and the initial distribution of velocity, $u(x, z, 0)$, was taken as independent of the depth and of magnitude given by the riverflow, q assumed to be constant, divided by the cross-sectional area (7). It was necessary to have a run-in period during which the salinity was unchanged from its initial distribution at 0600 hr

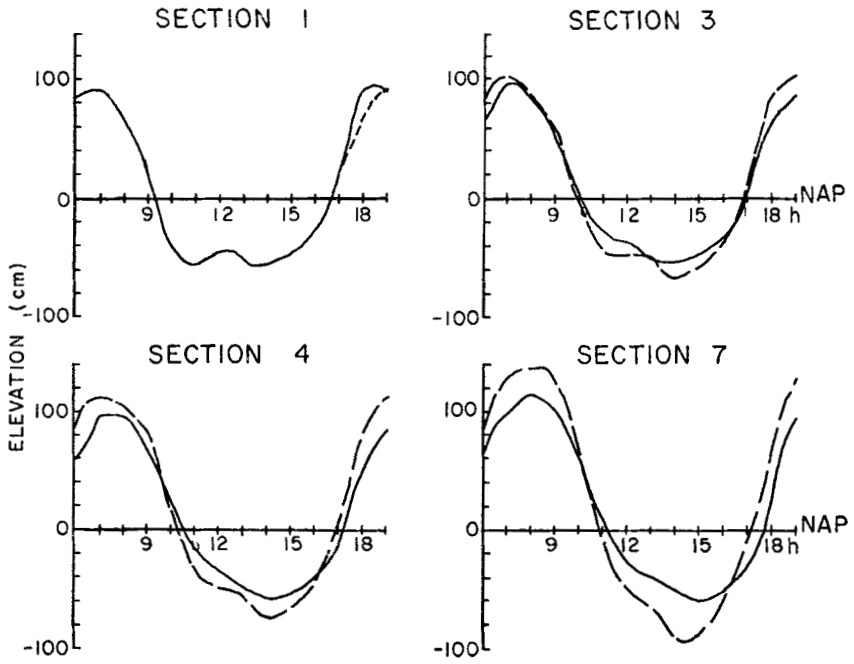

FIG. 6. Computed (— — — —) and measured (————) tidal elevations for Sections 1 (km 1029), 3 (km 1020·4), 4 (km 1015·6) and 7 (km 1002·1). The alteration to the tide at Section 1 for the run in tidal cycle is shown by (– – – – –). ($z = 0$ is taken to be the NAP datum for Rotterdam.)

so as to allow the velocity field and elevations to adjust to the pressure field. This adjustment in quite rapid (2–3 hr of real time), however, a run-in period of 12·5 hr was used, corresponding to one tidal period during which the estuary was driven by the tidal elevation at the mouth. This was taken to be the same as the period 0600–1830 hr with the curve slightly altered so that it returned to its starting value at the end of the period (Fig. 6). This procedure allows direct comparison of the data with the results from the period when the salinity is allowed to advect and diffuse. These results are less likely to be affected by artificial initial values used for the velocity field than if the model had only been run for one period.

The quantities used in the computations are:

$$\left.\begin{aligned} L &= 99\,\text{km},\\ b &= 400\,\text{m},\\ h &= 13\,\text{m},\\ \delta &= 2\,\text{m},\\ \varepsilon &= 2\,\text{km},\\ \tau &= 1\,\text{min},\\ q &= 1000\,\text{m}^3\,\text{s}^{-1}\\ K_z &= 5\,\text{cm}^2\,\text{s}^{-1},\\ K_x &= 0\,\text{cm}^2\,\text{s}^{-1}, \end{aligned}\right\} \qquad (43)$$

$$N_z = 5+0{\cdot}5\times10^{-3}H|\bar{u}|(1+7Ri)^{-\frac{1}{2}}\,\mathrm{cm^2\,s^{-1}} \tag{44}$$

where H is the total depth of water, $\bar{u}$ is the depth mean velocity at any instant and Ri is the depth mean Richardson number, given by

$$Ri = \frac{ag\Delta s/H}{(0{\cdot}7\bar{u}/H)^2} \tag{45}$$

with Δs being the top to bottom salinity difference.

The functional form of N_z was chosen as a result of experiments performed with a hypothetical channel of simple geometry, representative of a coastal plain estuary such as the Mersey, to investigate the effects on the circulation of different functional forms for the eddy coefficients. These experiments will be described in a further paper. It was found that if N_z is a function of the tidal current, the qualitative behaviour of current and salinity distribution had a better correspondence with measurements particularly at high and low water where an increase in the stratification and shear is apparent in the measurements. The dependence of N_z on Ri, and hence the overall stratification, also gives a better representation of the differences found between ebb and flood tides. On the flood the stratification (i.e. Δs in (45)) tends to be smaller than on the ebb. This is found in the model results even if a constant value of N_z is used, so the dependence of N_z on Ri in (44) reduces the values of N_z on the ebb, producing greater shear in the current which is more in accordance with the observations. The maximum value of N_z on the ebb is approximately half that on the flood tide. This difference between ebb and flood values of N_z is also shown in the measurements of Bowden, Fairbairn & Hughes (1959). The coefficients used for the dependence of N_z on Ri were derived from Bowden & Gilligan's (1971) results for the Mersey. The coefficient $0{\cdot}5\times10^{-3}$ in (44) gives a reasonable representation of the data and is the same order as in Pritchard's formula for K_z, deduced from tidal mean data for the James River (Pritchard 1960).

Initially a similar formulation for K_z was used

$$K_z = 5+0{\cdot}5\times10^{-3}H|\bar{u}|(1+Ri)^{-7/4}\,\mathrm{cm^2\,s^{-1}}. \tag{46}$$

However, the values of K_z given by the model did not produce the right degree of stratification and it appears that turbulent diffusion is suppressed by the vertical salinity gradient to a greater extent than allowed by (46). The best results were found by holding K_z constant. A major problem in estuaries is the interdependence of K_z and N_z and their dependence on local variables such as current and stratification. Further work, using a hypothetical channel, has been carried out using formulations similar to (44) and (46) which give some insight into the tidal behaviour of estuarine circulations and will be the subject of a further paper.

The horizontal diffusion coefficient K_x has been neglected in this study, mainly because little information is available about its magnitude and behaviour and also because only one or two tidal periods are considered here. If the model is used to represent a large number of periods (say 20) then a horizontal diffusion coefficient is necessary because the salt balance in most coastal plane estuaries is not entirely due to advection, and there is a significant fraction due to upstream diffusion of salt (Hansen & Rattray 1965). The difficulty of choosing a value of K_x which will maintain an approximate longitudinal salt balance is compounded by the fact that an apparent K_x already exists due to the finite difference form of the advective terms in (3) (Section 4). The loss of salt through the seaward boundary due to the riverflow is small enough to be neglected for the time considered here.

The most important terms in the dynamical equations are the pressure term involving the horizontal density gradient and the vertical friction term. The inertial terms are relatively unimportant. In the salt balance equation, the terms in order of

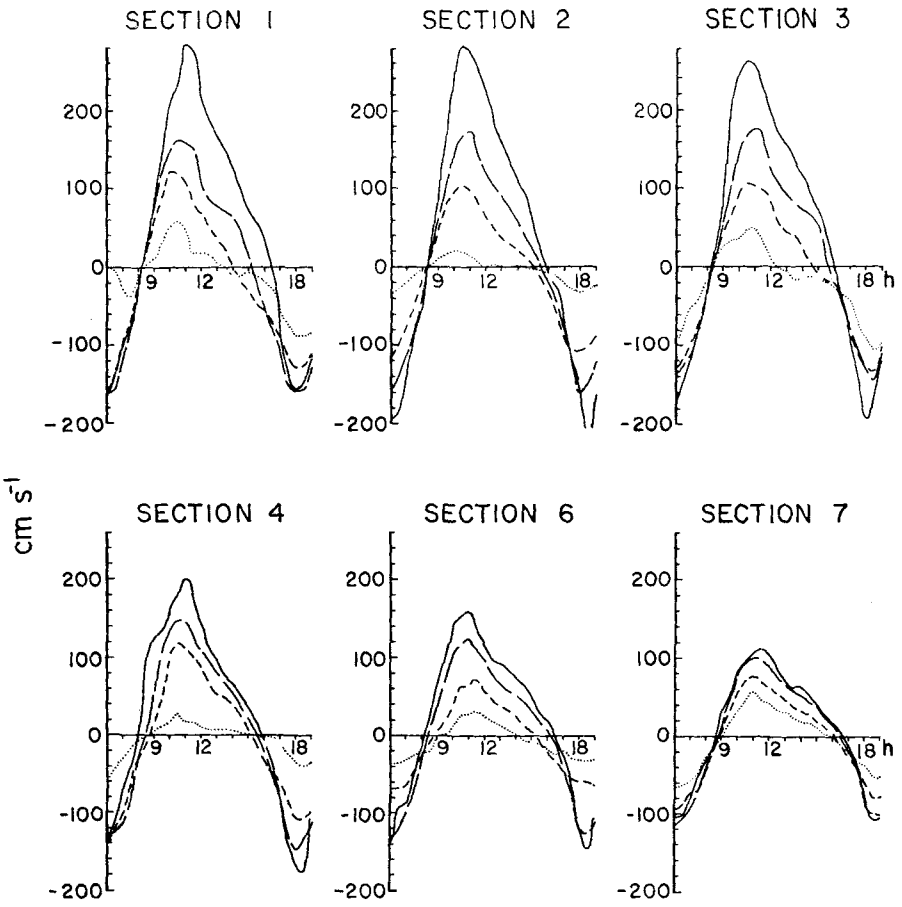

FIG. 7. Width mean measured velocities at depths $(n-\frac{1}{2})\delta'$ below the water surface, where $\delta' = (H+\zeta)/H \cdot 2$ m, H = depth below NAP and ζ = elevation, for Sections 1 (km 1029, $H = 15$ m, $n = 1, 4, 6, 8$), 2 (km 1024·6, $H = 13$ m, $n = 1, 3, 5, 7$), 3 (km 1020·4, $H = 13$ m, $n = 1, 3, 5, 7$), 4 (km 1015·6, $H = 14 \cdot 6$ m, $n = 1, 4, 6, 8$), 6 (km 1008·2, $H = 11 \cdot 1$ m, $n = 1, 3, 5, 6$) and 7 (km 1002·1, $H = 11 \cdot 7$ m, $n = 1, 3, 5, 6$). ———— $n = 1$ (surface); — — — — $n = 3$ or 4; – – – – – – $n = 5$ or 6; · · · · · · $n = 6$, 7 or 8 (bottom).

importance are the horizontal advection term, the vertical diffusion term and almost equally with this, the vertical advection term.

Fig. 6 shows the computed and measured tidal elevations at Sections 3, 4 and 7. It can be seen that the measured tidal wave is rather more damped than the computed wave and this is probably due to the dissipative effect of the extensive docks and harbours on the Waterway. Vreugdenhill (1970) uses a 'storage width' of 600 m to overcome this, however, this has not been done for this model. Apart from this, agreement, particularly in the lower reaches, is quite good.

The velocity-time graphs for Sections 1, 2, 3, 4, 6 and 7 derived from the measurements, by averaging across the width of the channel, are shown in Fig. 7. The computed values, taken from the nearest columns of grid points to the sections, are given in Fig. 8. It can be seen that the features of the data are qualitatively reproduced and for Sections 1–3, the magnitudes and phases correspond quite well. For Sections 4, 6 and 7 the computed velocities have higher peak values on the ebb tide than the measurements, though the flood velocities are about right, which can be attributed

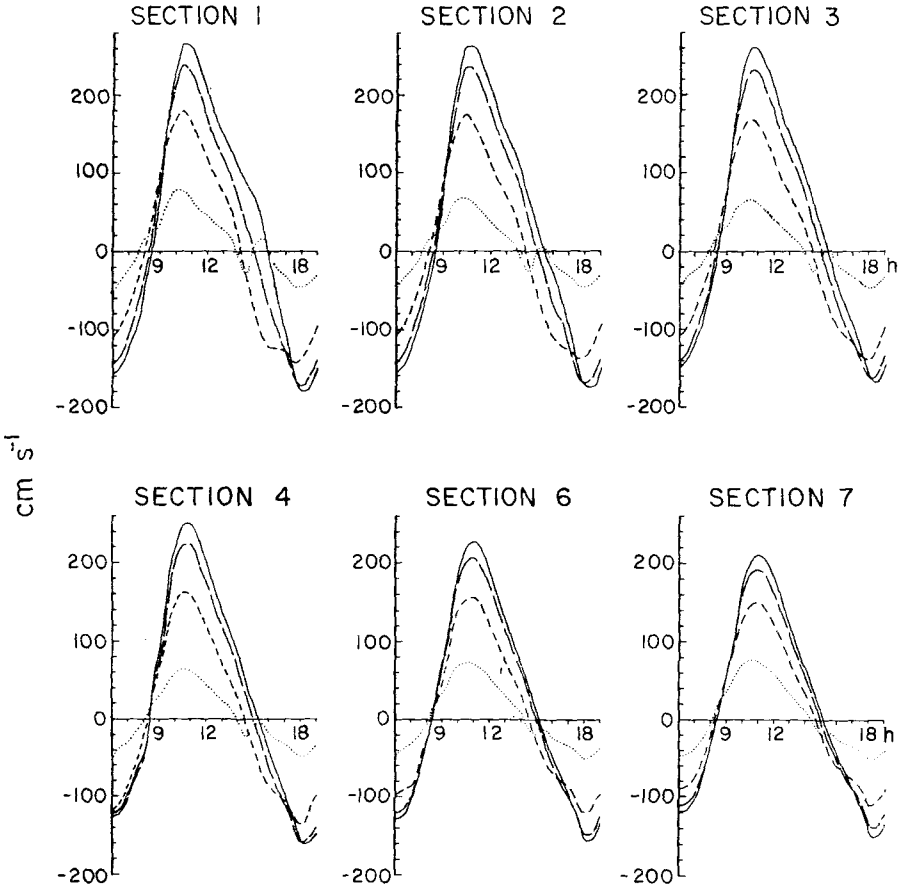

FIG. 8. Computed velocities at depths $(n-\frac{1}{2})\delta'$ below the water surface where $\delta' = (H+\zeta)/H \cdot 2$ m, $H = 13$ m, ζ = elevation, for the velocity columns $p = 50, 48, 46, 44, 40$ and 37 which correspond to Sections 1, 2, 3, 4, 6 and 7 respectively. ———— $n = 1$ (surface); — — — — $n = 3$; - - - - - - $n = 5$; · · · · · · $n = 7$ (bottom).

to the range of the computed tide at these sections as noted above. The effect of the large horizontal density gradient is apparent in the strong shear of the ebb velocities particularly after 1100 hr and the reduced shear of the flood velocities. The computed velocities have smaller vertical gradients near the surface than the measured velocities, which is probably due to using a depth independent form for N_z. It is probable that N_z reduces in value towards the surface which would increase the amount of shear there (Bowden, Fairbarn & Hughes 1959). Velocity profiles obtained from Vreugdenhill's (1970) two-layer model also tend to have smaller gradients than the measured ones.

Fig. 9 shows surface, depth mean and bottom salinities derived from the measurements. The features are the degree of stratification at all times, but particularly on the ebb tide (1100–1700) and the large differences between maximum and minimum salinities over the period. The computed salinities from the columns of grid points corresponding to Sections 2, 3, 4, 6 and 7 are given in Fig. 10. Again there is qualitative agreement with the measured salinities. Particularly noteworthy is the reduction in the salinity ranges between Sections 4 and 6, however, in all the sections the surface

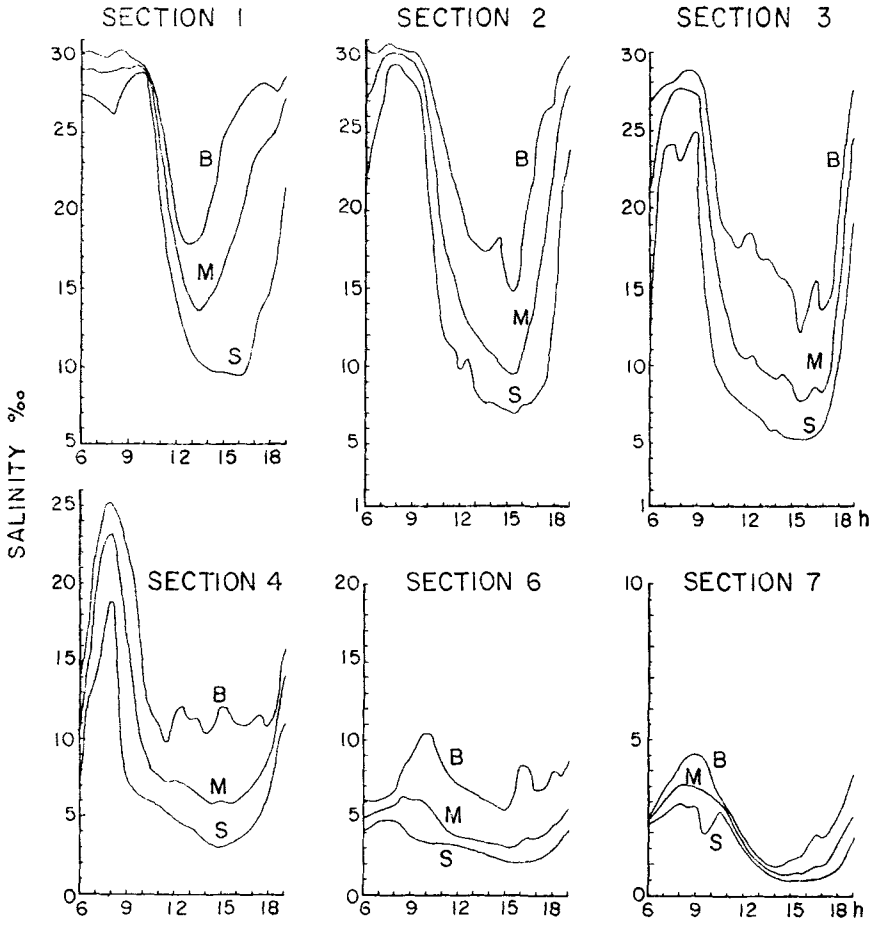

FIG. 9. Width mean measured surface (S), bottom (B) and depth mean (M) salinities at Sections 1, 2, 3, 4, 6 and 7.

salinity falls too low on the ebb tide. Vreugdenhill observed the same effect in the version of his model which allows mixing between the two layers. An explanation of this may lie in the neglect of the horizontal salt diffusion term in equation (3). Increasing the vertical diffusion coefficient K_z reduces the degree of stratification and still produces salinities which are too low.

However, given that calculations have been carried out for an idealized channel and that the Rotterdam Waterway is a severe test of any mathematical model, it is felt that a reasonable representation of the tide, currents and salinities has been obtained, even though the lack of knowledge on the behaviour of the eddy coefficients is a limiting factor.

8. Conclusions

A numerical model has been constructed to calculate the vertical distribution of current and salinity along with the tidal elevation throughout a tidal period. The equations are solved by a finite difference scheme, using forward and backward differences in time arranged so that the scheme is essentially explicit. The grid on which the finite difference equations are solved is arranged in the vertical plane and is

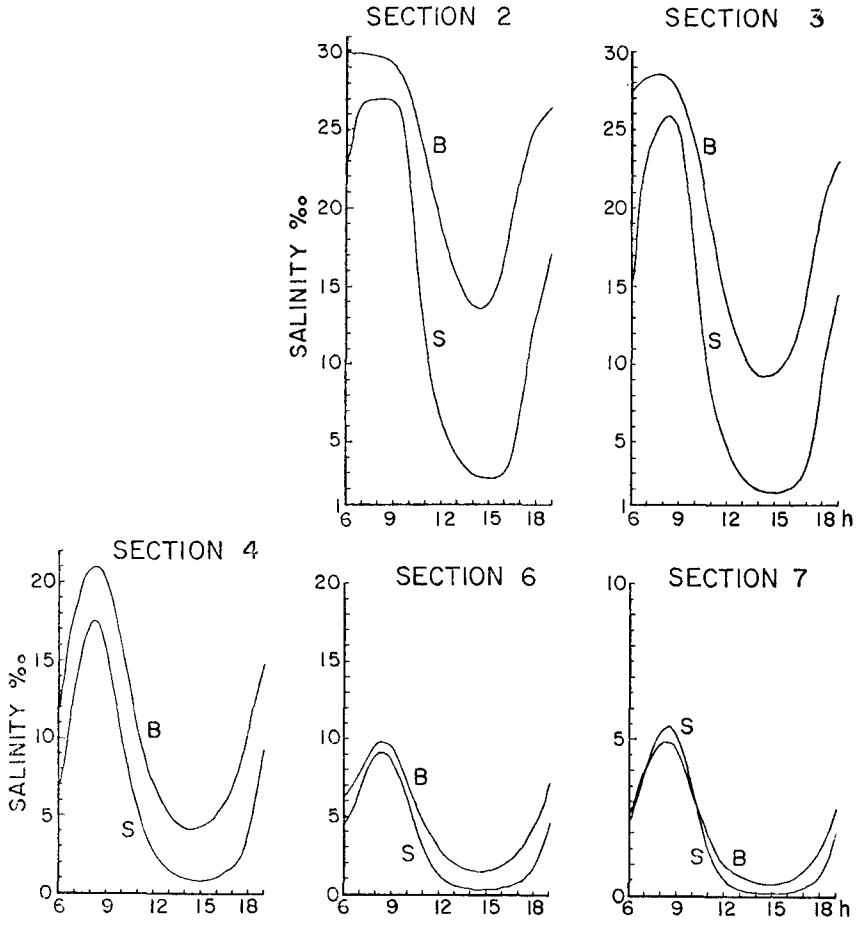

FIG. 10. Computed surface (S) and bottom (B) salinities for salinity columns p = 48, 46, 43, 40 and 37 corresponding to Sections 2, 3, 4, 6 and 7, respectively.

similar to that employed by Heaps (1969). Several features are noteworthy, among them the movement of the free surface through the grid points and the methods of including the boundary conditions in the finite difference equations. The model was designed as a research tool and the results of experiments with a hypothetical channel will be the subject of a further paper. The model has been used to reproduce the situation in the Rotterdam Waterway and the results compared with field data. The agreement is satisfactory considering the nature of the Waterway and the use of an idealized channel to model it. To this extent, therefore, the ability of the model to reproduce the features of estuarine circulation in a tidal estuary has been established.

Acknowlegments

This work was carried out while I was at Liverpool University and I should like to record my thanks to Professor K. F. Bowden for suggesting the development of this type of model and for his support and interest throughout the work. I am grateful to Dr N. S. Heaps for a number of helpful discussions on the numerical model during its development. Also my thanks to the late Dr J. J. Dronkers and his colleagues at

the Rijkswaterstaat at the Hague for providing the data from their surveys of the Rotterdam Waterway must be recorded. This work was supported by a Natural Environment Research Council Studentship and is contribution 807 from the Department of Oceanography, University of Washington.

Department of Oceanography,
University of Washington,
Seattle, Washington 98195, *USA.*

References

Arakawa, A., 1966. Computational design for long term numerical integration of the equations of fluid motion. Two-dimensional incompressible flow. Part 1, *J. comp. Phys.*, **1,** 119–143.

Birkhoff, G. & Garabedian, H. C., 1960. Smooth surface interpolation, *J. Math. Phys.*, **39,** 258–268.

Boor de, C., 1962. Bicubic spline interpolation, *J. Math. Phys.*, **41,** 212–218.

Bowden, K. F., 1967. *Circulation and diffusion. Estuaries.* Ed. G. H. Lauff, American Association for the Advancement of Science, New York.

Bowden, K. F., Fairbairn, L. A. & Hughes, P., 1959. The distribution of shearing stresses in a tidal current, *Geophys. J. R. astr. Soc.*, **2,** 288–305.

Bowden, K. F. & Gilligan, R. M., 1971. Characteristic features of estuarine circulation as represented in the Mersey estuary, *Limn. Oceanogr.*, **16,** 490–502.

Chan, R. K–C. & Street, R. L., 1970. Computer study of finite amplitude water waves, *J. comp. Phys.*, **6,** 68–94.

Crowley, W. P., 1968. Numerical advection experiments, *Mon. Weath. Rev.*, **96,** 1–11.

Daly, B. J. & Pracht, W. E., 1968. A numerical study of density current surges, *Phys. Fluids*, **11,** 1–15.

Dronkers, J. J., 1964. *Tidal computations in rivers and coastal waters*, John Wiley & Sons, New York.

Fromm, J. E., 1968. A method for reducing dispersion in convective difference schemes, *J. comp. Phys.*, **3,** 176–189.

Hamilton, P., 1973. *A numerical model of the vertical structure of tidal estuaries*, Ph.D. thesis, University of Liverpool.

Hansen, D. V. & Rattray, Maurice, 1965. Gravitational circulation in straits and estuaries, *J. mar. Res.*, **23,** 104–122.

Heaps, N. S., 1969. A two-dimensional numerical sea model, *Phil. Trans. R. Soc. A*, **265,** 93–137.

Hobbs, G. D. & Fawcett, A., 1973. Two-dimensional estuarine models, *Proc. Symp. Math. Hydro. Mod. Estuarine Poll.* Water Pollution Research, Tech. paper 13, 127–137, Department of the Environment, London, HMSO.

Leendertse, J. J., 1967. Aspects of a computational model for long-period water wave propagation, *Memor. Rand Corp.*, Santa Monica, Calif. RM–5294–PR.

Leendertse, J. J., 1970. A water quality simulation model for well-mixed estuaries and coastal seas. Vol. 1, *Principle of Computation. Memor. Rand Corp.*, Santa Monica, Calif. RM–6230–RC.

Mollowney, B. M., 1973. One-dimensional models of estuarine pollution, *Proc. Symp. Math. Hydr. Mod. Estuarine Poll.*, Water Pollution Research, Tech. paper 13, 72–83, Department of the Environment, HMSO, London.

Morton, K. W., 1971. Stability and convergence in fluid flow problems, *Proc. R. Soc. A*, **323,** 237–253.

Nichols, B. D. & Hirt, C. W., 1971. Improved free surface boundary conditions for numerical incompressible flow calculations, *J. comp. Phys.*, **8,** 434–448.

Pritchard, D. W., 1956. The dynamic structure of a coastal plain estuary, *J. mar. Res.*, **15,** 33–42.

Pritchard, D. W., 1960. The movement and mixing of contaminants in tidal estuaries, *Proc. 1st Intern. Conf. on Waste Disposal in the Marine Environment*, University of California at Berkley, Pergamon Press Inc., New York.

Richtmyer, R. D. & Morton, K. W., 1967. *Difference methods for initial value problems*, Interscience Publ., New York.

Roach, P. J., 1972. On artificial viscosity, *J. comp. Phys.*, **10,** 169–184.

Rossiter, J. R., 1961. Interaction between tide and surge in the Thames, *Geophys. J. R. astr. Soc.*, **6,** 29–53.

Rossiter, J. R. & Lennon, G. W., 1965. Computation of tidal conditions in the Thames by the initial value method, *Proc. Inst. Civ. Engrs. (London)*, **31,** 25–56.

Stigter, C. & Siemons, J., 1967. Calculation of longitudinal salt-distribution in estuaries as a function of time, *Delft Hydraulics Laboratory*, Publ. No. 52.

Vreugdenhill, C. B., 1970. Computation of gravity currents in estuaries, *Delft Hydraulics Laboratory*, Publ. No. 86.

Williams, D. J. A. & West, J. R., 1973. A one-dimensional representation of mixing in the Tay Estuary, *Proc. Symp. Math. Hydr. Mod. Estuarine Poll.* Water Pollution Research, Tech. paper 13, 118–125, Department of the Environment, HMSO, London.

Young, J. A. & Hirt, C. W., 1972. Numerical calculation of internal wave motion (2-D stratified flows), *J. fluid Mech.*, **56,** 256–276.